08 May 1984, 10:15 am - 5:00 pm

Performance of Trial Embankment on Soft Clay

T. Shibata
Kyoto University, Kyoto, Japan

H. Sekiguchi
Kyoto University, Kyoto, Japan

Performance of Trial Embankment on Soft Clay

T. Shibata
Professor, Kyoto University, Kyoto, Japan

H. Sekiguchi
Associate Professor, Kyoto University, Kyoto, Japan

SYNOPSIS This paper is concerned with the interpretation of the observed and predicted performances of a full-scale trial embankment, which was constructed for the design purposes regarding a new bypass road to be constructed over soft clay adjacent to existing structures. The prediction based on the finite element analyses and the determination of soil parameters are briefly outlined. The results of comparison show adequate agreement between the predicted and observed field time-dependent deformation behavior throughout the entire loading history. However, if the predictions from the present FE-analyses are made by using the soil parameters measured in the laboratory, a correction factor of 6 on the value of coefficient of consolidation is required to obtain reasonable agreement with the field behavior. Finally, the practical suggestions are made for assessing the effect on the nearby existing structures of soil movements towards the outside of embankment.

INTRODUCTION

The national highway program has led to the construction of a 9.3 km-long bypass between the districts of Ohnishi and Agasaki of Kurashiki City, Okayama Prefecture, Japan. The principal role of the bypass (called Tamashima bypass) is to mitigate an increasingly heavy traffic on the existing highway (Route No.2), especially in the rapidly populated districts of Tamashima City.

Geotechnically, the construction of Tamashima bypass called for practical solutions to the following problems: one was concerned with the stability of embankment sections to be constructed on soft deposits of alluvial clay; and the other was concerned with the deformation problem described below.

The route design of Tamashima bypass required an embankment section to pass alongside several private houses, with a very tight distance between the embankment and those houses. It was also required that, in another site for a solid crossing, the ramp embankment should pass alongside very near the existing railroad. Thus, concern had been expressed over possible influences on such nearby structures of the soil movements to be caused by the embankment loads. Furthermore, from cost considerations, a feasibility of the method of slowly embanking with no resort to soil improvements was asked to be assessed urgently.

Thus, the Okayama office for Highway Construction of the Ministry of Construction decided to construct a trial embankment (called Kurashiki trial embankment), to assist in the design of all embankment sections, which include the most difficult sections mentioned above.

An account of the measured performance of Kurashiki trial embankment has previously been given by Mochizuki et al. (1980). The corresponding predictions from an analysis based on the method of finite elements have briefly been described by Sekiguchi and Shibata (1982).

In what follows, a detailed review of the measured and predicted performances of Kurashiki trial embankment will be made, with particular emphasis on clarifying the practical significance and predictability of the lateral soil movements.

KURASHIKI TRIAL EMBANKMENT

Plan and elevation views of Kurashiki trial embankment are given in Fig.1. It is located in a flooded plain of river Takahashi, which flows through Kurashiki City into Seto Inland Sea. The elevation of the test site is T.P. ±0 m, indicating it to be located in a typical soft ground area. It is also known that the test site was once a reclaimed land in the late Edo Era.

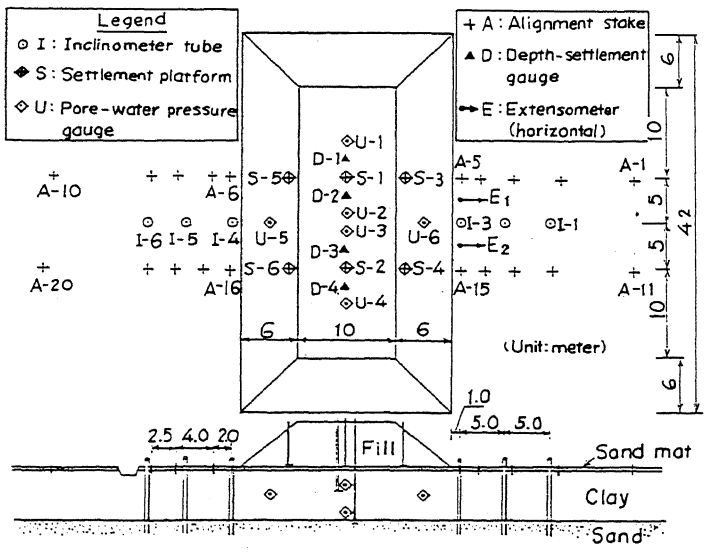

Fig. 1. Plan and elevation of trial embankment

A top 0.4 m of the test site is covered with a sand mat which was placed on the original ground surface about 1 year before the commencement of trial embanking. A soft layer of alluvial clay extends from a depth of 0.4 m from the current ground surface to a depth of 6.3 m and is underlain by a thick layer of diluvial sand. The diluvial sand, with several intermittent diluvial clay layers, extends to a depth of 33.4 m and is underlain by a sand-and-gravel layer resting on the base rock.

The embanking was performed over a 42 m by 22 m rectangular area to a height of 5.0 m from the top surface of the sand mat, by using a residual soil of granitic origin called 'masa'. The rate of embanking was maintained at 0.1 m/day until a height of 3.9 m was reached. Then, a short rest time period of 6 days was taken. The embanking was resumed at t=45 days and was completed at t= 57 days. After its completion, the embankment was left to stand until the final readings were taken at t=161 days.

It should be mentioned here that the factor of safety of Kurashiki trial embankment at the end of construction had been estimated by the engineer in charge to be 1.18, from a series of before-event analyses using the classical method of a slip circle.

Field instrumentation consisted of six settlement platforms (base depth is 0 m), four depth-settlement gauges (base depth is either 3.0 m or 7.0 m), twenty alignment stakes, six inclinometer tubes, two horizontal extensometers, and six electric pore-water pressure gauges (tip depth is either 2.0 m or 3.0 m or 5.0 m). It will be evident from Fig.1 that the field instrumentation was aimed at precisely measuring the soil movements below and, in particular, outside the embankment.

SOIL PROPERTIES

A thin-walled sampling was made prior to construction, in the center of the test site. The obtained samples were used for classification, strength and consolidation tests.

The results of the classification tests are shown in Figs. 2(a) and (b). It is seen from Fig. 2 that the clay contains and increasing fraction of sand as the top or bottom surface of that layer is approached. This feature is in good agreement with the distributions with depth of the natural water content (w_n) and of the liquid limit (w_L).

The strength tests consisted of unconfined compression tests, unconsolidated-undrained triaxial tests, and consolidated-drained triaxial tests. The values of undrained shear strength (s_u) obtained from the conventional strength tests, are plotted against depth in Fig. 2(c). While there is a considerable scatter in the s_u versus depth relation, it may be possible to get a rough estimate of s_u=2 tf/m² (19.6 kPa). Indeed, this value had been used in the afore-mentioned stability analyses. The results from the consolidated-drained triaxial tests will be explained later in due course.

Figure 2(d) shows the preconsolidation pressure σ_{vc}' versus depth relation, which was obtained

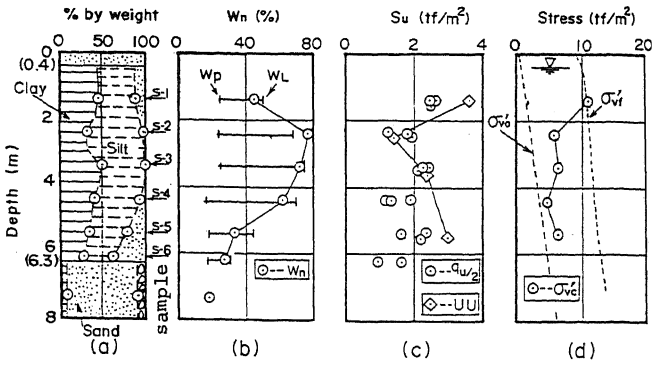

Fig. 2. Soil properties

from the standard oedometer tests. For the purpose of comparison, a plot of σ_{vo}' as well as σ_{vf}' against depth is also made in Fig. 2(d). Here, σ_{vo}' is the initial effective overburden pressure, and σ_{vf}' is the final effective vertical stress which has been estimated based on the elastic stress distribution. It is seen from this figure that the foundation clay is in state of light to moderate overconsolidation. It is also seen that approximately all the clay will be brought into normally-consolidated states when its consolidation under the full embankment loading has been completed.

The compressibility of the foundation clay in the standard oedometer tests is shown in Fig. 3, where void ratio (e) is plotted against effective vertical stress (σ_v'), not against log (σ_v'). The arrows marked on Fig. 3 stand for the points of yielding, which were determined by following the Casagrande's procedure. It is seen that the current procedure permits a reasonable estimate of σ_{vc}' except for the sand-rich sample S-6.

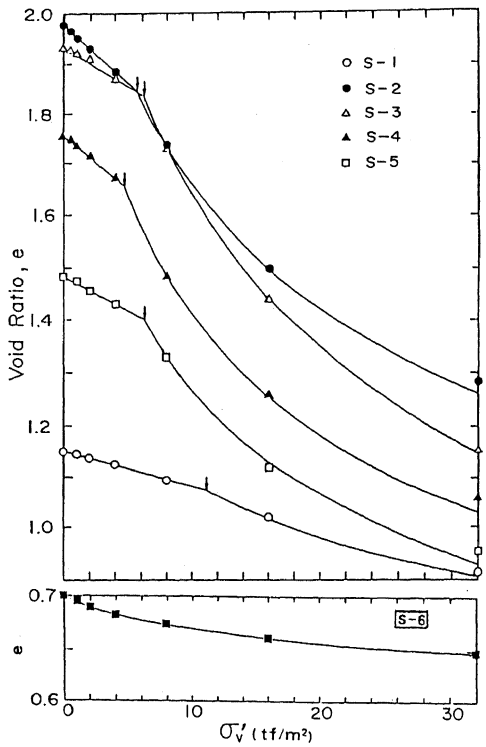

Fig. 3. Results of oedometer tests

The coefficients of vertical consolidation (c_v) determined from the standard oedometer tests on the foundation clay, are plotted against logarithm of (σ_v') in Fig. 4. It is seen that the coefficient of consolidation of a given sample tends to decrease rapidly as its preconsolidation pressure σ_{vc}' is exceeded, except the case of sand-rich sample S-6.

The results shown in Figs. 3 and 4 permit the coefficient of vertical permeability (k_v) to be expressed as a function of void ratio (e), such as shown in Fig. 5. Then, it follows that

$$e = e_o + \lambda_k \ln (k_v/k_{vo}) \qquad (1)$$

where e_o is a reference void ratio, k_{vo} is the coefficient of permeability at $e=e_o$, and λ_k is a soil constant governing the rate of change in permeability with void ratio. Note here that $\lambda_k=0.434C_k$ by definition.

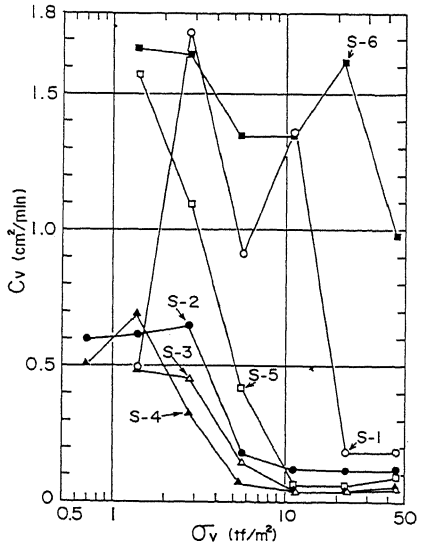

Fig. 4. Variation of coefficient of consolidation with vertical stress

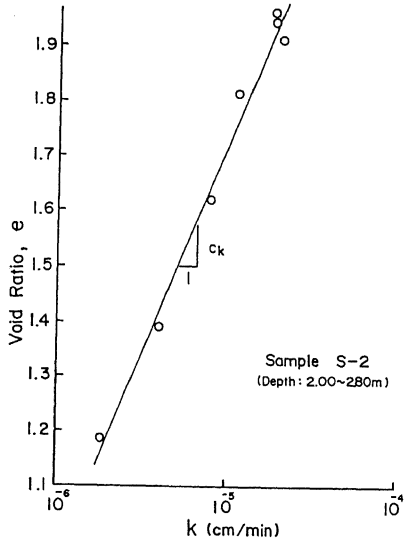

Fig. 5. Void ratio vs coefficient of vertical permeability

Another advantage of the standard oedometer testing is to permit us to gain information on volumetric creep characteristics of the clay under study, such as shown in Fig. 6. Here, α is the coefficient of secondary compression and is defined by

$$\alpha = dv/d \ln(t) = 0.434\, C_\alpha/(1 + e_o) \qquad (2)$$

where v is the volumetric strain and C_α is the coefficient of secondary compression in terms of void ratio (e). In the authors' analyses described later, the coefficient of secondary compression α is assumed to be zero in states of overconsolidation, while, in normally consolidated states, it is assumed to take a constant value, irrespectively of consolidation pressure.

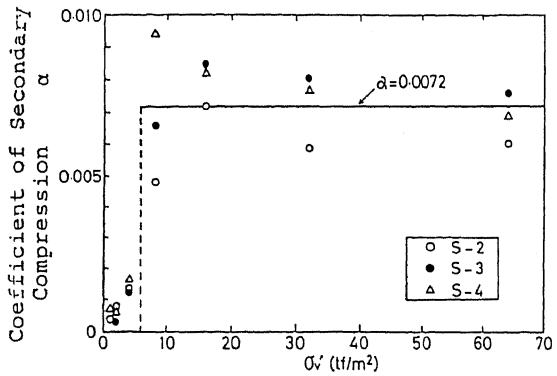

Fig. 6. Coefficient of secondary compression vs vertical stress

Two series of consolidated-drained tests were performed by the authors to determine the friction constant (M) of the foundation clay. In Series I, all the samples were isotropically consolidated at the same pressure of 20 tf/m² (196 kPa) and were brought into normally consolidated states before shearing. It is seen from Fig. 7 that the stress-strain curves of the samples S-2, S-3 and S-4 show a typical soft clay behavior, while those of the sand-rich samples S-5 and S-6 show a reduced compressibility and an associated higher shear resistance. The sample

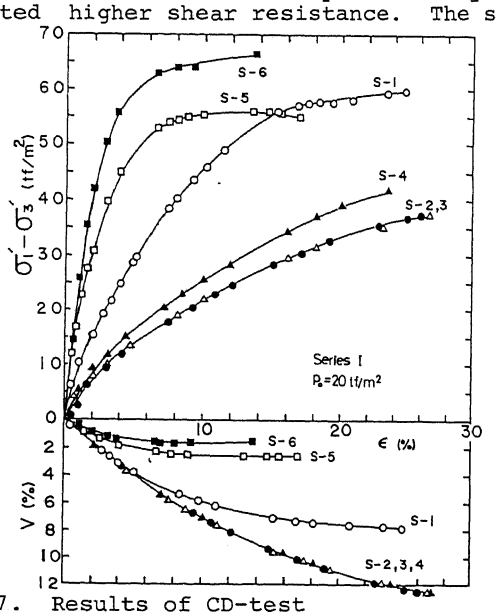

Fig. 7. Results of CD-test

S-1 shows an intermedate pattern of stress-strain behavior. The effective stress states at failure are plotted in Fig. 8, together with the data points from Series II with consolidation pressures different from 20 tf/m² (196 kPa).

Note here that the friction constant (M) is related to the angle of friction in terms of effective stress ϕ' as follows (Schofield and Wroth, 1968):

$$M = \frac{6 \sin\phi'}{3 - \sin\phi'} \quad (3)$$

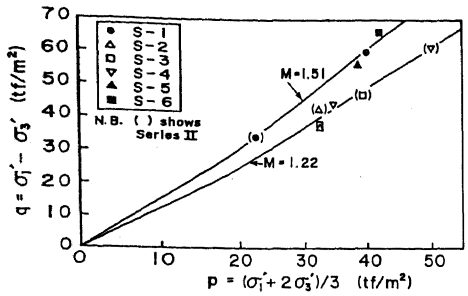

Fig. 8. Effective stress states at failure

FINITE ELEMENT ANALYSIS

Introduction

In the course of interpreting the measured performance of Kurashiki trial embankment, it was soon revealed that current method of analysis have serious limitations in clarifying the integrated nature of the field soil behavior, especially with respect to the contained plastic flow under partially-drained conditions. This had led the authors to perform their analyses using the method of finite elements so as to gain a deeper insight into the performance of the soft clay under the trial embankment loading.

Features of the analysis performed

One features of the analysis performed is that it treats the foundation clay as a two-phase material. The constitutive behavior of the soil skeleton is assumed to obey the elasto-viscoplastic model (Sekiguchi, 1977) and is implemented into the finite element program through the following form of constitutive relations:

$$\{\Delta\sigma'\} = [C]\{\Delta\varepsilon\} - \{\Delta\sigma^r\} \quad (4)$$

where $\{\Delta\sigma'\}$ stands for a set of effective stress increments, $\{\Delta\varepsilon\}$ stands for a set of strain increments, and $[C]$ is the coefficient matrix depending on the current effective stress state as well as on the amount of viscoplastic volumetric strain. The term $\{\Delta\sigma^r\}$ represents a set of effective stress increments which are to be relaxed with time when strains are held constant. For details of Eq. (4), reference should be made to Shibata and Sekiguchi (1980) or Sekiguchi et al. (1981).

The pore-water flow is assumed to obey the generalized Darcy's law having the coefficients of permeability k_v and k_h. Here, k_v and k_h are the vertical and horizontal coefficients of permeability, respectively, both of which are assumed to vary with the change in void ratio (refer to Eg. (1)).

Another feature of the present analysis is to permit a proper simulation of construction procedure of the trial embankment, with due consideration of the fill rigidity.

The finite element mesh adopted in the present analysis is shown in Fig. 9, together with the imposed boundary conditions. Perfect drainage is assumed for the fill material throughout. The finite elements used are quadrilateral elements, each of which consists of four constant-strain triangular elements. The nodal displacement increments and element pore-water pressure are taken to be the primary unknowns. The basic equations governing those unknowns are derived based on the so-called Biot's formulation, with particular reference to the works of Christian (1968) and of Akai and Tamura (1976). The finite element equations are then assembled in matrix form in each step of calculation and solved by means of a semi-bandwidth method of Gaussian elimination (Desai and Abel, 1972).

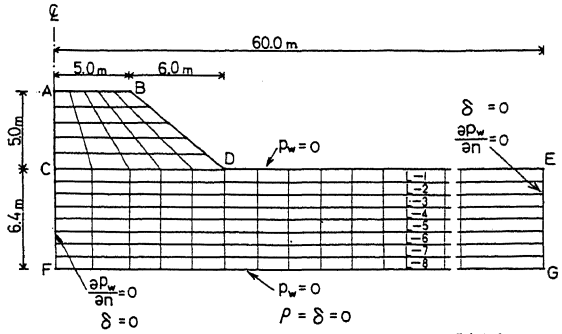

Fig. 9. FE-mesh and boundary conditions

The sequence of embanking adopted in the presen analysis is shown in Fig. 10. The element gene ration for the embankment is made every one met of filling at a prescribed time, as indicated b an arrow. Furthermore, to simulate more closel the actual embanking procedure, we have sub-divided the body force increment of a newly gener ated element into five increments, such that ea of the sub-divided increments corresponds to th load to be caused by a 0.2 m-thick filling.

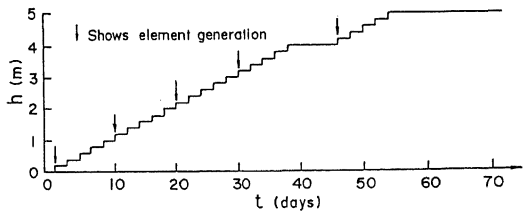

Fig. 10. Sequence of embanking

Soil parameters determined

The soil parameters determined for the present analysis are summarized in Table A-1 in the APPENDIX. Most of those values have been deter mined from the laboratory test results which ar shown in Figs. 2 through 8.

The unit weight of the embankment (γ) was measu ed in-situ to be 1.85 tf/m³ (18.1 KN/m³). The linear elastic model is assumed for the fill ma rial for the purpose of simplification. The value of Young's modulus (E') for the fill mate rial was reported to be 500 tf/m² (4.9 MPa).

This value was obtained from a series of in-situ pressuremeter testing with the fill, with Poisson's ratio ν' being assumed to be 0.3 throughout. This set of elastic moduli leads to a value of G=190 tf/m^2 (1.9 MPa), which is listed in Table A-1. Here, G is the modulus of shear rigidity.

COMPARISON BETWEEN MEASURED AND PREDICTED PERFORMANCE

Back-analysis of field permeability

The measured performance of Kurashiki trial embankment has shown taht the embankment settled at much more larger rates than those which had been predicted from a conventional one-dimensional analysis with c_v being obtained from standard oedometer tests (Mochizuki et al., 1980). This feature has been confirmed by the authors based on their finite element analyses, which result in:

$$(k_{vo})_{field} = 6\ k_{vo} \qquad (5a)$$

$$(k_{ho})_{field} = 6\ k_{ho} \qquad (5b)$$

where (k_{vo}) and (k_{ho}) are the laboratory-measured coefficients of permeability and their values are listed in Table A-1. Note here that the isotropic permeability as well as the constancy of the parameter λ_k have been assumed.

It should be emphasized here that the predicted performance stated below is entirely based on the analysis using such back-figured values of permeability. Therefore, the significance of the predicted performances should be judged, not from the degree of its agreement with the measured performances but from its consistency and integrity.

Settlement performances

Let us first discuss the performance of settlements (ρ) along the center-line of the embankment. The measured and calculated settlements of the ground surface are plotted against elapsed time in Fig. 11, together with the measured settlements of the base of soft clay. The chain-dotted curve stands for the average of the time-settlement histories of the depth settlement gauges D-2 and D-4. The dotted curve represents the predicted time-history of the ground settlement. By adding the afore-metioned base settlement for a given time, we can get the solid curve.

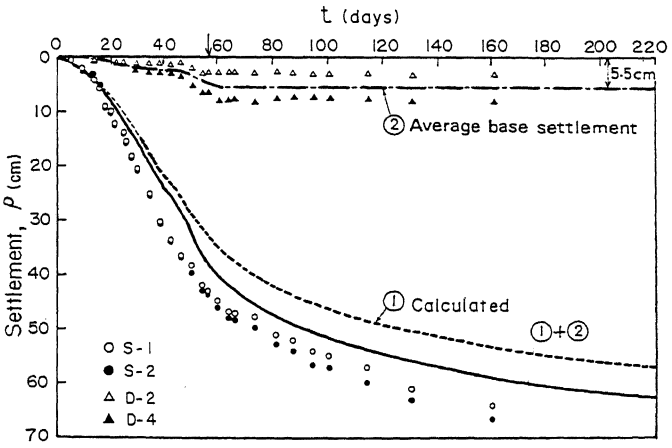

Fig. 11. Settlement under the center of embankment

An estimate for the final settlement obtained from the present analysis is 66.9 cm, with allowance of the base settlement of 5.5 cm. It is then seen from Fig. 11 that the measured settlements at the end of construction give rise to 62% of the final settlement in a very short time period of 57 days. This notable speed of field settlement has two consequences: first, the existence of some sort of macro-fabric in the soft clay is suggested; second, the rapid rate of consolidation under the field conditions confirms the feasibility of the slowly-embanking technique of construction which had been suggested in the early stage of design.

The measured settlement at three different depths at t=161 days are summarized in Fig. 12, together with the corresponding calculated curve. This figure also indicates the importance of taking into consideration the base settlement.

It may be appropriate here to mention that a conventional one-dimensional settlement analysis has provided a value of 55.0 cm for the final settlement, with allowance of the base settlement of 5.5 cm. It is seen that the conventional method of analysis predicts a somewhat smaller value of final settlement in this particular case history.

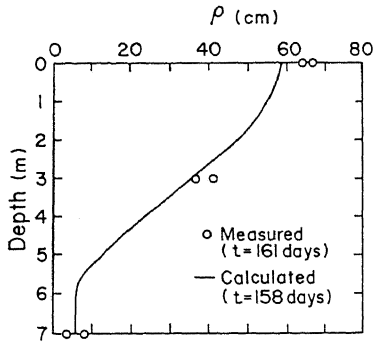

Fig. 12. Settlement profile under the center of embankment

Let us next discuss the surface settlement profile in the cross-sectional plane. Fig. 13 shows the measured settlement profiles at the end of construction and at the final readings, together with the corresponding calculated curves. Note here that allowance of base settlements is made in the manner such as shown in the inset of Fig. 13. It will be noted in Fig. 13 that both measured and calculated results show a rather small heave outside the embankment, even at the end of construction. This also suggests that significant consolidation has progressed during the construction period.

Furthermore, Fig. 13 shows that a marked settlements of the toe of embankment are predicted from the present analysis (i.e, 2.7 cm at the end of construction and 10 cm at t=158 days). This feature is considered to be a consequence of taking the fill rigidity into consideration and seems to be compatible with the stress transfer phenomena predicted (see Fig. 14).

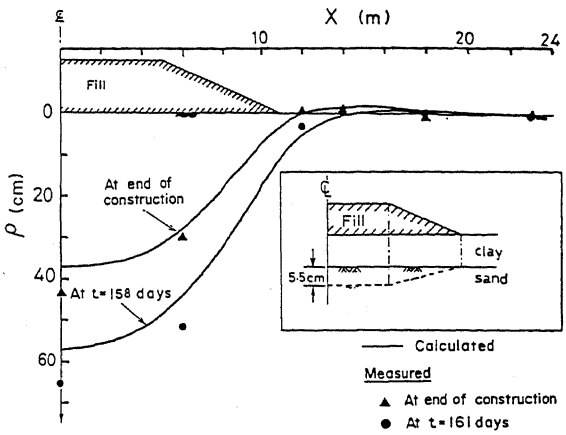

Fig. 13. Surface settlement profile in the cross-sectional plane

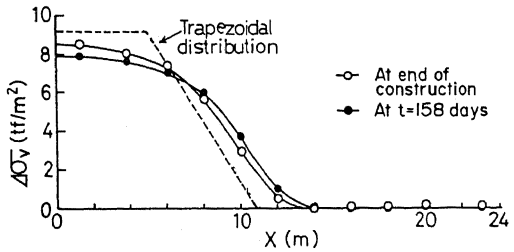

Fig. 14. Distribution of vertical stress increment with distance x, at a depth of 0.4 m

Performance of pore-water pressure

The measured and calculated excess pore-water pressure (p_w) are plotted against nominal embankment pressure (γh) in Fig. 15, where h stands for the embankment thickness. It is seen from Fig.15 that both measured and calculated p_w versus γh relations are situated far below the line of $p_w = \gamma h$. This again suggests the significant progress of consolidation during the construction stage.

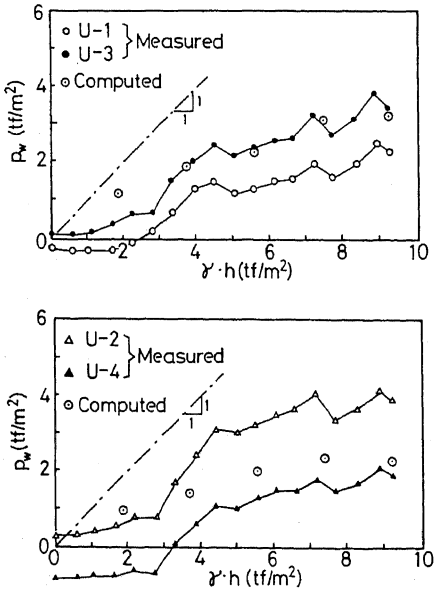

Fig. 15. Excess pore water pressure vs embankment pressure

This is furthermore reinforced by the results shown in Fig. 16, where pore-water pressures at the end-of construction are plotted against depth

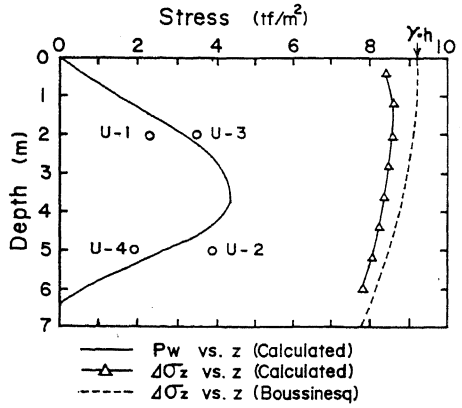

Fig. 16. Pore pressure profiles at the end of construction

Performance of lateral soil movement

In what follows, the lateral soil movement in the directions away from the embankment is taken as positive.

Before going into a detailed comparison of the measured and predicted performance of lateral soil movements, let us grasp a general trend observable in the measured performance. Fig. 17 presents a general picture showing the variations with space and time of the lateral displacements (δ) measured by means of the inclinometers I-4, I-5 and I-6. It is noted from Fig. 17(a) that, below the toe of embankment, the maximum lateral displacement occurs at a depth of 2.0 m for a given time. On the other hand, far outside the embankment (I-5 and I-6), the maximum lateral displacement is noted to occur at the ground surface for a given time, while its value decreases with increasing distance from the toe of embankment.

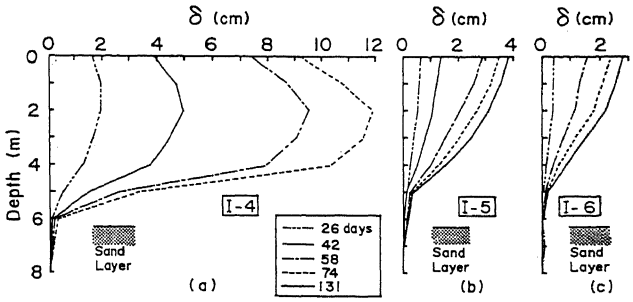

Fig. 17. Lateral displacements measured by inclinometers

Next, let us discuss the measured performance of surface lateral displacement at the toe of embankment, which was obtained from three sets of independent measuring devices: the inclinometer tubes (I-3, I-4); the alignment stakes (A-5, A-6, A-15, A-16) and the extensometers (E-1, E-2). The results from the inclinometer tubes and alignment stakes are shown in Fig. 18. It is seen that there is general agreement between the inclinometer data and those of the alignment stakes unti

the end-of-construction state is reached. Thereafter, however, the inclinometer tubes tend to give smaller values of lateral displacement than the alignment stakes do, at a given time of measurements. In this respect, it is anticipated that the inclinometer tubes were not able to accommodate to the lateral soil movements which developed rapidly just after the completion of embanking. It should also be mentioned that the extensometers gave almost the same time-histories of lateral displacement as the inclinometer tubes did.

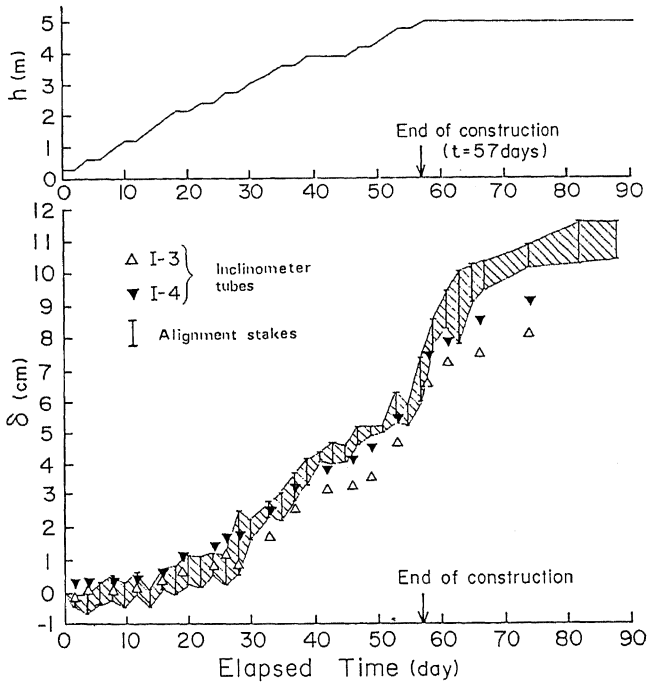

Fig. 18. Embankment height and measured lateral displacement

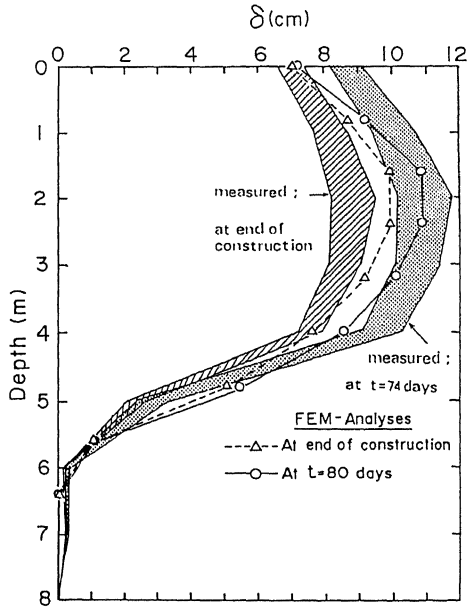

Fig. 19. Lateral displacement profiles, below the toe of embankment

Figure 19 shows the measured and calculated distributions of the lateral displacement with depth under the toe of embankment. It is seen that the shapes of the calculated and measured curves agree with each other, except for the top 1 m from the ground surface. One possible reason is the overestimation of fill rigidity in the present analysis. In relation to this, however, further study will be needed.

Rate of development of δ with ρ

It has been suggested by Tominaga and Hashimoto (1974) that the abrupt increase in $(\Delta\delta/\Delta\rho)$ is an indication of the instability of the embankment foundations, where (δ) is the surface lateral displacement at the toe and (ρ) is the settlement along the center-line of embankment.

In order to examine this more closely with reference to the measured performance of Kurashiki trial embankment, we have constructed Fig. 20. Here, the average of the lateral displacements measured at the toe of embankment using the four alignment stakes is plotted against the average settlement obtained from the two settlement platforms S-1 and S-2. As a result, the curve OABCD is formed. The corresponding, calculated curve is expressed as $\overline{OABCDE}$. The number in a pair of parentheses stands for the elapsed time in days. It is seen from Fig. 20 that the measured performance is characterized by the two features: the existence of a threshold around point A; and the rapid increase in $(\Delta\delta/\Delta\rho)$ just after the completion of embanking.

These two features seem to be related closely to the fact that the foundation clay was initially in states of light to moderate overconsolidation and has undergone yielding with increased effective stresses (see Fig. 2(d)). Thus, the authors believe that the foundation clay should have experienced a marginal condition of stability, at least for a while just after the completion of embanking.

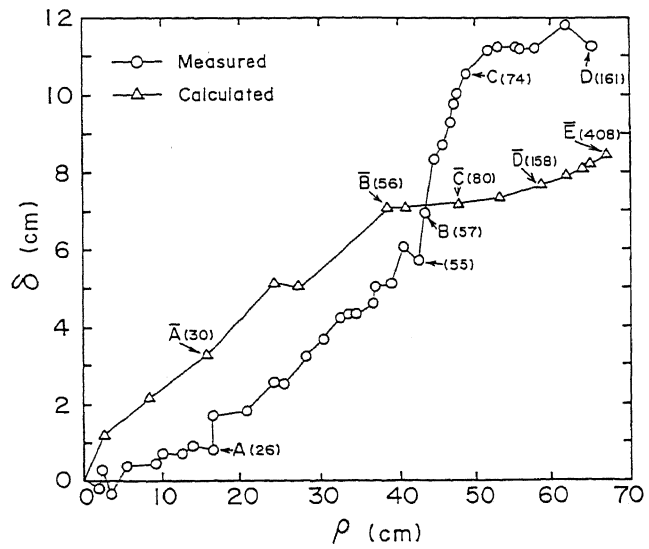

Fig. 20. Lateral displacement vs settlement during and after the construction

PRACTICAL SIGNIFICANCE OF SOIL MOVEMENTS OUTSIDE THE EMBANKMENT

One of primary objectives of Kurashiki trial embankment was to assess the rate of decay of soil movements outside the embankment. This assessment was essential to avoid detrimental effects of soil movements of the nearby existing structures, which include a national railroad and several private houses.

Figure 21 summarizes the measured lateral displacements along the ground surface, together with the corresponding, calculated curves. It is seen that, for a given time, the measured lateral displacements tend to decay more rapidly with the horizontal distance x (measured from the embankment axis) than do the predicted ones. This tendency will be understandable in view of the fact that the present analysis assumes the plane-strain soil behavior, while the actual soil behavior is three-dimensional, in particular, far outside the embankment.

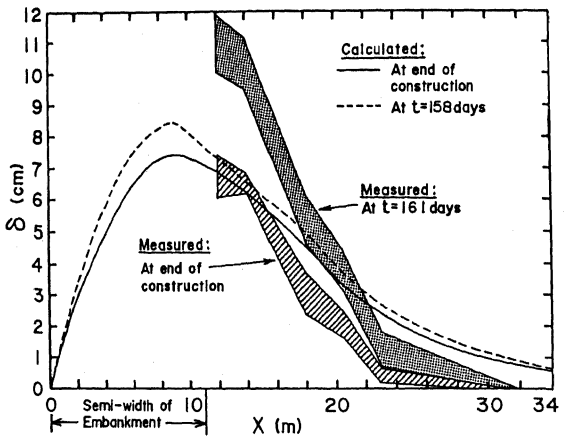

Fig. 21. Distributions of lateral displacement along the ground surface with distance x

From a practical point of view, such rapid decay of the observed lateral displacements is advantageous. If an upper limit of allowable lateral displacements is tentatively taken to be 2 cm, then the corresponding distance x is estimated to be 23 m (12 m away from the toe of embankment), based on the measured performance. If the plane-strain situation is assumed to occur, then the maximum distance of influence becomes x=25 m (14 m away from the toe of embankment), based on the predictions given in Fig. 21.

In order to reinforce the conclusions stated above, we have prepared Fig. 22, where distributions of the vertical movement of the ground surface outside the embankment are summarized. It is seen from Fig. 22 that,in the region with x being larger than 23 m, the measured settlement amounts to the order of 0.5 cm, whereas the predicted vertical movement ranges from -0.5 cm to almost zero. Thus, in this particular embankment, the extent of the deformation-affected region is assessed to be within 14 m outside the embankment (i.e, $x \leq 25$ m).

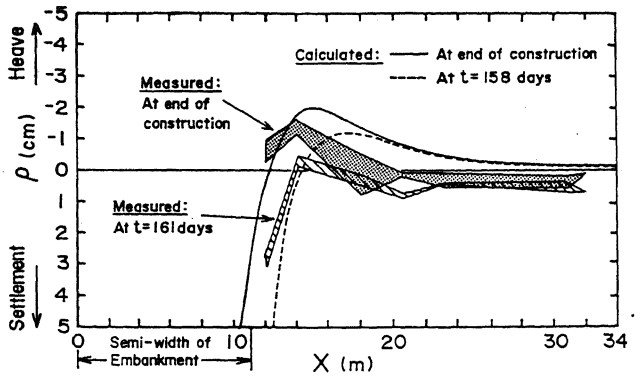

Fig. 22. Distributions of vertical movement of the ground surface with distance x

CONCLUSIONS

The measured performance of Kurashiki trial embankment has been reviewed in detail in the light of the predicted performance based on the finite element analyses. The principal conclusions drawn are summarized as follows.

(1) The back-analyzed field rates of consolidation are six times as large as those predicted from a conventional one-dimensional analysis using the laboratory-measured coefficients of consolidation.

(2) The above-mentioned conclusion has two consequences: First, the rapid rates of consolidation under the field conditions are very beneficial from a practical point of view and confirm the feasibility of slowly embanking technique, with no resort of soil improvements, which had been suggested in the early stage of design; Second, the above-mentioned finding emphasizes again that practical methods of properly determining the field permeability should be developed urgently, in order that the before-event predictions using the method of finite elements become really adequate.

(3) The present finite element analyses show that the measured abrupt increase in $\Delta\delta/\Delta\rho$ just after the completion of embanking does not contradict the above-mentioned rapid rates of consolidation, but is compatible with the actual changes in soil state, from overconsolidated to normally-consolidated states, which should have been experienced by the foundation clay under the full embankment loads.

(4) The results shown in Figs. 21 and 22 make it possible to assess the extent of deformation-affected region to be within 14 m outside the embankment (i.e, $x \leq 25$ m).

APPENDIX

The soil parameters used in the present finite element analyses are summarized in Table A-1.

Table A-1

Element in Fig.9	Model *	G (tf/m^2)	ν'	λ	κ	M	α	$\dot{v}_0$ (d^{-1})	k_{vo} (m/d)	$\frac{k_{ho}}{k_{vo}}$	λ_k
Embank.	A	190	0.30	–	–	–	–	–	–	–	–
L-1	A	92	0.30	–	–	1.51	–	–	3.2×10^{4}	1.0	∞
L-2	B	92	0.30	0.16	0.054	1.51	0.0039	4×10^{-5}	3.1×10^{-4}	1.0	0.10
L-3	B	49	0.27	0.36	0.24	1.22	0.0072	4×10^{-5}	2.7×10^{-4}	1.0	0.32
L-4	B	49	0.27	0.36	0.24	1.22	0.0072	4×10^{-5}	2.6×10^{-4}	1.0	0.32
L-5	B	49	0.27	0.36	0.24	1.22	0.0072	4×10^{-5}	1.4×10^{-4}	1.0	0.32
L-6	B	49	0.27	0.36	0.24	1.22	0.0072	4×10^{-5}	1.4×10^{-4}	1.0	0.32
L-7	B	49	0.27	0.29	0.20	1.51	0.0061	4×10^{-5}	3.1×10^{-4}	1.0	0.18
L-8	A	150	0.27	–	–	1.51	–	–	2.4×10^{-4}	1.0	∞

*A=linear elastic, B=elasto-viscoplastic

ACKNOWLEDGEMENTS

The valuable field measured data used in this analysis were furnished by the Okayama Office for Highway Construction of the Ministry of Construction to which the authors are deeply indebted. Thanks are also due to Mr. Y. Morita, engineer of Kiso-Jiban Consultants Co. LTD, who supervised the field observations.

PREFERENCES

Akai, K. and T. Tamura (1976), "An Application of Nonlinear Stress-Strain Relations to Multi-dimensional Consolidation Problem", Annuals, Disaster Prevention Research Institute, Kyoto University, No. 21 B-2, 19-35 (in Japanese).

Christian, J. T. (1968), "Undrained Stress Distribution by Numerical Methods", Journal of Soil Mechanics and Foundation Division, ASCE, Vol. 94, No. SM6 1333-1345.

Desai, C. S. and J. F. Abel (1972), Introduction to the Finite Element Method, 477 pp., Van Nostrand Reinhold Company, New York, USA.

Mochizuki, K., T. Hiroyama, Y. Morita and A. Sakamaki (1980), "The Measured Performance of Lateral Soil Movements in Kurashiki Trial Embankment", Proc., 15th Annual Meeting on Soil Mechanics and Foundation Engineering, Japanese Society of Soil Mechanics and Foundation Engineering, 861-864 (in Japanese).

Schofield, A. N. and C. P. Wroth (1968), Critical State Soil Mechanics, 310 pp., McGraw-Hill, London, UK.

Sekiguchi, H. (1977), "Rheological Characteristics of Clays", Proc., 9th International Conference on Soil Mechanics and Foundation Engineering, Tokyo, Vol. 1, 289-292.

Sekiguchi, H., Y. Nishida and F. Kanai (1981), "Analysis of Partially-Drained Triaxial Testing of Clay", Soils and Foundations, Vol. 21, No. 3, 53-66.

Sekiguchi, H. and T. Shibata (1982), "Lateral Displacement Prediction for Soft Clay Foundation below a Trial Embankment", TSUCHI-TO-KISO, Japanese Society of Soil Mechanics and Foundation Engineering, Vol. 30, No. 5, 47-54 (in Japanese).

Shibata, T. and H. Sekiguchi (1980), "A Method of Predicting Failure of Embankment Foundation Based on Elasto-Viscoplastic Analyses", Proceedings of the Japan Society of Civil Engineers, No. 301, 93-104 (in Japanese).

Tominaga, M. and M. Hashimoto (1974), "Stability Control for Embankments by Measuring Lateral Soil Movements", TSUCHI-TO-KISO, Japanese Society of Soil Mechanics and Foundation Engineering, Vol. 22, No. 11, 43-51 (in Japanese).